



UNIVERSITÀ
DEGLI STUDI
FIRENZE

FLORE

Repository istituzionale dell'Università degli Studi di Firenze

Squeeze flow of a Bingham-type fluid with elastic core

Questa è la Versione finale referata (Post print/Accepted manuscript) della seguente pubblicazione:

Original Citation:

Squeeze flow of a Bingham-type fluid with elastic core / Fusi, Lorenzo; Farina, Angiolo; Rosso, Fabio. - In: INTERNATIONAL JOURNAL OF NON-LINEAR MECHANICS. - ISSN 0020-7462. - STAMPA. - 78(2016), pp. 59-65. [10.1016/j.ijnonlinmec.2015.10.004]

Availability:

This version is available at: 2158/1008031 since: 2021-03-27T12:11:32Z

Published version:

DOI: 10.1016/j.ijnonlinmec.2015.10.004

Terms of use:

Open Access

La pubblicazione è resa disponibile sotto le norme e i termini della licenza di deposito, secondo quanto stabilito dalla Policy per l'accesso aperto dell'Università degli Studi di Firenze (<https://www.sba.unifi.it/upload/policy-oa-2016-1.pdf>)

Publisher copyright claim:

(Article begins on next page)

Squeeze Flow of a Bingham-Type Fluid with Elastic core

L. Fusi, A. Farina, F. Rosso
Università degli Studi di Firenze
Dipartimento di Matematica “U. Dini”
Viale Morgagni 67/a, 50134 Firenze, Italy

July 16, 2015

Abstract

The squeeze flow of a Bingham-type material between finite circular disks is considered. The material is modelled assuming that the unyielded region behaves like a linear elastic core. A lubrication approximation is considered. It is shown that no paradox can arise, such as that has been pointed out for many years by various authors when the unyielded region in the fluid is supposed to be perfectly rigid. The unyielded region is shown to be always detached from the axis of symmetry. Some numerical simulations are worked out for different squeezing rates.

1 Introduction

The squeeze flow between circular discs is often encountered in many devices used to determine the flow properties of highly “viscous” materials such as concrete, molten polymers, ceramic pastes etc. Most of these materials are constitutively modeled as Bingham plastics [1], that is continua associated to a “plastic” criterion (Von Mises) that links the stress state and the yield stress. If the criterion is satisfied, a velocity gradient arises in the medium and the body starts to flow as a linear viscous fluid. If the criterion is not fulfilled, there is no velocity gradient and the material is stationary or moves as a rigid plug [2].

In many situations the geometrical setting of the problem is such that the aspect ratio is negligibly small, so that lubrication approximation can be used, see [3]. While, on the one hand, lubrication allows for major simplifications of the governing equations, on the other, it may cause the emergence of paradoxes and inconsistencies that invalidate the main constitutive assumptions. As stated by Covey et al. [3] and subsequently by Wilson in [4], there is an immediate difficulty when one deals with Bingham squeeze lubrication flow as the expected yield surface clashes with the model. Indeed, simple symmetry arguments require that the shear stress (which is dominant) decreases below the yield stress close to the mid-plane. Hence, the flow criterion is not fulfilled there and an unyielded region forms around the mid-plane. Because of the cylindrical geometry, the plug has to be stationary, but, at the same time, the gap between the plates is being narrowed and the plug has to deform. The solution thus becomes inconsistent and a paradox arises.

This result, that was first pointed out by Lipscomb and Denn in [5], led the authors to argue that true rigid plug cannot exist in complex geometries, since the lubrication scaling predicts unyielded plugs that move with a velocity that slowly varies in the principal flow direction (the so called

pseudo-plugs, see [6], [7]). Though the paradox remains true for axisymmetric squeeze flow, in many other complex geometries asymptotic solutions that predict truly rigid regions have been found. Balmforth et al. [8] have proposed a procedure that allows to construct consistent solutions for thin-layer problems, a technique subsequently exploited by Frigaard et al. [9] for the Bingham flow in a channel of slowly varying width.

In the last decades many ways of overcoming the “lubrication paradox” paradox have been developed. For example Gartling et al. [10] and Wilson [4] have proposed to substitute the original Bingham model with a bi-viscous model in which the solid behaviour is never required even for zero shear rate. Others [11], [12] have used exponential viscosity models or power-law fluid models [13], [14]. We refer the readers to [15], [16], [17], [18], [11], where a vast literature on such an issue can be found. In particular an exhaustive review of the regularization models and their implementation can be found in [19], while an excellent review on yield stress fluids can be found in [20]. Recently Fusi et al. [21] have proposed a new procedure where the rigid plug is treated as an evolving non-material volume and where the momentum balance of the unyielded region is written through an integral formulation. This procedure allows to determine a true plug at the leading order of the lubrication approximation with no need to define pseudo-plug or fake yield surface. The same approach has been used in Fusi et al. [22] to study the squeeze flow of a Bingham fluid in planar geometry. In the paper by Muravleva [23] the planar squeeze flow is studied following the technique introduced in Balmforth et al. [8] and Frigaard et al. [9]. In the specific case of axisymmetric squeeze flow Smyrniotis et al. [11] have shown that unyielded material may exist only around stagnation points located at the center of the disks and their results are confirmed by numerical simulations.

In this paper, following an approach developed in [24], [25], we consider the axisymmetric squeeze flow of a Bingham-like material. and we overcome the lubrication paradox by modelling the material as a Bingham fluid with a deformable core. In particular we model the unyielded domain as a linear elastic solid, but other constitutive relations can be used. By doing this we allow the solid plug to deform and no paradox arises at the mid-plane placed between the plates. In practice we are considering a yield stress fluid which behaves like a linear elastic solid when the stress is below a fixed threshold. We remark that the idea of modelling the core as an elastic material dates back to the works by Oldroyd [2], and by Yoshimura and Prud’homme [26]. However, to our knowledge, such a model was never applied to the squeezing between circular discs.

We consider the continuum confined between two parallel discs, both of radius¹ R^* , moving one toward the other in a prescribed way thus causing the squeezing of the fluid (Fig. 1). Denoting by $h^*(t^*)$ the half distance between discs, we assume

$$\varepsilon = \frac{R^*}{H^*} \ll 1, \quad H^* = \sup_{t^* \geq 0} h^*(t^*), \quad \frac{dh^*}{dt^*} \leq 0, \quad (1.1)$$

so that the lubrication approximation is justified. We assume that the material behaves as a linear viscous fluid if the stress is above a critical threshold τ_o^* and as a linear elastic solid when stress state is below τ_o^* . We develop the mathematical model at the leading order and show that the model predicts the existence of an evolving yield surface which, however, appears only after some time depending on the squeezing velocity. After the emergence of the yield surface the domain is split in two regions: (i) an elastic domain where the material is unyielded; (ii) a sheared domain where the critical stress is overcome.

We will show that, at the leading order of the lubrication approximation, the region around the axis of symmetry remains always unyielded, so that the viscous region is always detached from that axis. We will perform some numerical simulation for different given expressions of the squeezing rate plotting the evolution of the yield surface and of the pressure profile.

¹Throughout the paper starred quantities indicate dimensional quantities.

2 The Mathematical model

Let us consider a mechanically incompressible continuum occupying a domain like the one depicted in Fig. 1. Suppose that two circular plates of radius R^* are squeezing the fluid confined in between and are approaching each other with prescribed motion $\pm h^*(t^*)$, with $\pm h^*(0) = \pm H^*$. As a consequence, the material is squeezed out radially. In radial polar coordinates² the displacement is given by

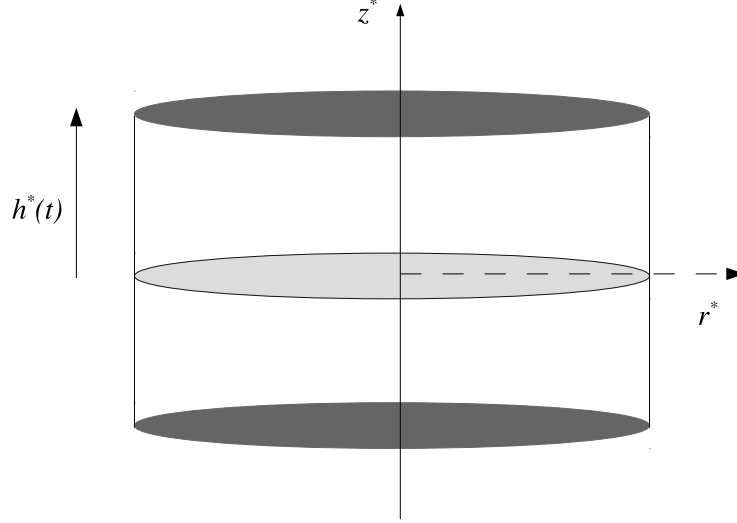


Figure 1: A schematic representation of the system.

$$\mathbf{u}^* = u_r^*(r^*, z^*, t^*)\mathbf{e}_r + u_z^*(r^*, z^*, t^*)\mathbf{e}_z, \quad (2.1)$$

while velocity is expressed by

$$\mathbf{v}^* = v_r^*(r^*, z^*, t^*)\mathbf{e}_r + v_z^*(r^*, z^*, t^*)\mathbf{e}_z, \quad (2.2)$$

We also assume that the displacement is *small* (infinitesimal strain theory), so that the Lagrangian description and the Eulerian description are essentially the same.

Being $\mathbf{T}^* = -p^*\mathbf{I} + \mathbf{S}^*$ the Cauchy stress tensor, $p^* = (1/3) \text{tr } \mathbf{T}^*$ the pressure, as in [24] we make the following constitutive assumption for the deviatoric part of \mathbf{T}^* :

$$\left\{ \begin{array}{ll} II_S^* < \tau_o^*, & \mathbf{S}^* = \left(2\eta^* + \frac{\tau_o^*}{II_D^*} \right) \mathbf{D}^*, \quad \text{viscous model,} \\ II_S^* < \tau_o^*, & \mathbf{S}^* = 2k^* \mathbf{E}, \quad \text{linear elastic model,} \\ II_S^* = \tau_o^*, & \text{yield condition,} \end{array} \right. \quad (2.3)$$

where:

$$\mathbf{D}^* = \frac{1}{2} \left[\overset{*}{\nabla} \mathbf{v}^* + (\overset{*}{\nabla} \mathbf{v}^*)^T \right], \quad \mathbf{E} = \frac{1}{2} \left[\overset{*}{\nabla} \mathbf{u}^* + (\overset{*}{\nabla} \mathbf{u}^*)^T \right],$$

²We assume no deformation/velocity in the θ -direction, as well radial symmetry, that is all relevant variables are independent of the polar coordinate θ .

- $II_S^* = \left[\frac{1}{2} \mathbf{S}^* \cdot \mathbf{S}^* \right]^{1/2}$ and $II_D^* = \left[\frac{1}{2} \mathbf{D}^* \cdot \mathbf{D}^* \right]^{1/2}$ are, respectively, the second invariant of \mathbf{S}^* and \mathbf{D}^* ,
- η^* is the viscosity of the fluid, τ_o^* the stress yield threshold and k^* the elastic modulus of the solid phase.

In practice the constitutive model (2.3) represents a Bingham-like material which behaves as a linear elastic body when $II_S^* < \tau_o^*$, and as a linear viscous fluid as $II_S^* > \tau_o^*$.

Mass balance is given by

$$\frac{\partial v_z^*}{\partial z^*} + \frac{\partial v_r^*}{\partial r^*} + \frac{v_r^*}{r^*} = 0, \quad (2.4)$$

while momentum conservation in the absence of body force is expressed by

$$\begin{cases} \rho \left(\frac{\partial v_r^*}{\partial t^*} + v_r^* \frac{\partial v_r^*}{\partial r^*} + v_z^* \frac{\partial v_r^*}{\partial z^*} \right) = -\frac{\partial p^*}{\partial r^*} + \frac{1}{r^*} \frac{\partial}{\partial r^*} (r^* S_{rr}^*) + \frac{\partial S_{rz}^*}{\partial z^*} - \frac{S_{\theta\theta}^*}{r^*}, \\ \rho \left(\frac{\partial v_z^*}{\partial t^*} + v_r^* \frac{\partial v_z^*}{\partial r^*} + v_z^* \frac{\partial v_z^*}{\partial z^*} \right) = -\frac{\partial p^*}{\partial z^*} + \frac{1}{r^*} \frac{\partial}{\partial r^*} (r^* S_{rz}^*) + \frac{\partial S_{zz}^*}{\partial z^*}. \end{cases} \quad (2.5)$$

The second invariant of \mathbf{S}^* writes

$$II_S^* = \left[\frac{1}{2} \mathbf{S}^* \cdot \mathbf{S}^* \right]^{1/2} = \sqrt{\left[S_{rz}^{*2} + \frac{1}{2} (S_{rr}^{*2} + S_{\theta\theta}^{*2} + S_{zz}^{*2}) \right]}. \quad (2.6)$$

The non-zero components of \mathbf{D}^* and \mathbf{E}^* are

$$D_{rr}^* = \left(\frac{\partial v_r^*}{\partial r^*} \right), \quad D_{zz}^* = \left(\frac{\partial v_z^*}{\partial z^*} \right), \quad D_{\theta\theta}^* = \left(\frac{v_r^*}{r^*} \right), \quad D_{rz}^* = \frac{1}{2} \left(\frac{\partial v_r^*}{\partial z^*} + \frac{\partial v_z^*}{\partial r^*} \right), \quad (2.7)$$

$$E_{rr} = \left(\frac{\partial u_r^*}{\partial r^*} \right), \quad E_{zz} = \left(\frac{\partial u_z^*}{\partial z^*} \right), \quad E_{\theta\theta} = \left(\frac{u_r^*}{r^*} \right), \quad E_{rz} = \frac{1}{2} \left(\frac{\partial u_r^*}{\partial z^*} + \frac{\partial u_z^*}{\partial r^*} \right), \quad (2.8)$$

whereas the second invariant of \mathbf{D}^* is more conveniently written as

$$II_D^* = \frac{1}{2} \left[\left(\frac{\partial v_r^*}{\partial z^*} \right)^2 + \left(\frac{\partial v_z^*}{\partial r^*} \right)^2 + 4 \left[\left(\frac{\partial v_r^*}{\partial r^*} \right)^2 + \left(\frac{v_r^*}{r^*} \right)^2 + \left(\frac{\partial v_r^*}{\partial r^*} \cdot \frac{v_r^*}{r^*} \right) \right] + 2 \left(\frac{\partial v_r^*}{\partial z^*} \cdot \frac{\partial v_z^*}{\partial r^*} \right) \right]^{1/2},$$

the above expression being obtained exploiting the mass conservation equation (2.4).

Because of symmetry we confine ourselves to the region $\{z^* > 0, r^* > 0\}$ and assume the existence of a sharp interface $z^* = \sigma^*(r^*, t^*)$ where $II_S^* = \tau_o^*$ (i.e. the yield surface, see Fig. 2), separating the viscous and elastic domain. We also assume that the flow is fully developed after a transient initial phase.

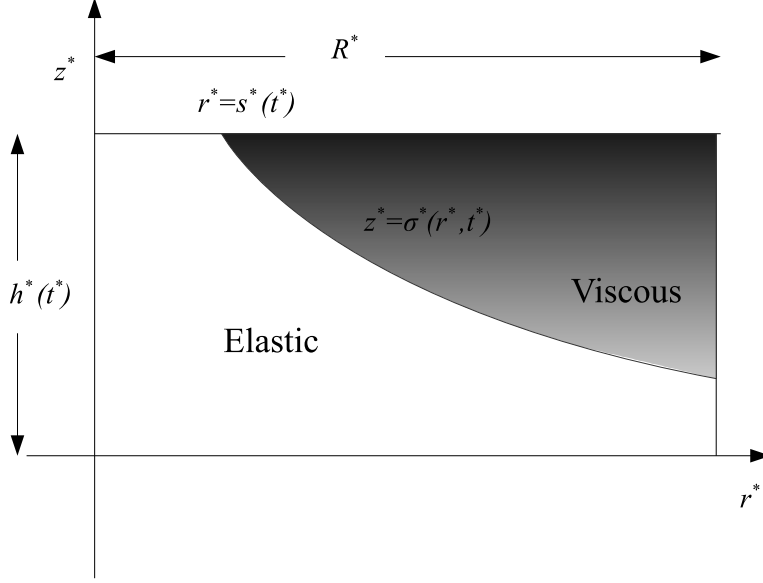


Figure 2: Viscous and elastic domain.

3 Boundary conditions

We write here the boundary conditions for the domain depicted in Fig. 2. Following [16] we write³

$$\begin{cases} v_z^* = \dot{h}^*(t^*), & v_r^* = 0, & (\text{no slip}), & \text{on } z^* = h^*(t^*), \\ v_z^* = 0, & S_{rz}^* = 0, & (\text{symmetry}), & \text{on } z^* = 0, \\ v_r^* = 0, & S_{rz}^* = 0, & (\text{symmetry}), & \text{on } r^* = 0, \\ p^* = P_{\text{out}}^* & & (\text{prescribed pressure}) & \text{at } r^* = R^*. \end{cases} \quad (3.1)$$

On the yield surface $z^* = \sigma^*(r^*, t^*)$, following [24], we impose the Rankine-Hugoniot conditions:

$$[\mathbf{v} \cdot \mathbf{t}] = 0, \quad [\mathbf{v} \cdot \mathbf{n}] = 0, \quad [\mathbf{Tn} \cdot \mathbf{t}] = 0, \quad [\mathbf{Tn} \cdot \mathbf{n}] = 0, \quad (3.2)$$

where \mathbf{n} , \mathbf{t} represent the normal and tangential unit vectors to σ^* . Conditions (3.2) rewrite explicitly as follows

$$\begin{cases} [[v_z^*]] = [[v_r^*]] = 0, \\ \left[\left[\left(\frac{\partial \sigma^*}{\partial r^*} \right)^2 T_{rr}^* - 2 \left(\frac{\partial \sigma^*}{\partial r^*} \right) T_{rz}^* + T_{zz}^* \right] \right] = 0, \\ \left[\left[- \left(\frac{\partial \sigma^*}{\partial r^*} \right) T_{rr}^* + \left[1 - \left(\frac{\partial \sigma^*}{\partial r^*} \right)^2 \right] T_{rz}^* + \left(\frac{\partial \sigma^*}{\partial r} \right) T_{zz}^* \right] \right] = 0, \end{cases} \quad (3.3)$$

where $[[\cdot]]$ denotes the jump across the interface $z^* = \sigma^*(r^*, t^*)$.

³The symbol $(\dot{\cdot})$ denotes the time derivative.

4 Non-dimensional formulation

We re-scale the variables of the problem in the following way ,

$$\mathbf{S}^* = \left(\frac{\eta^* U^*}{H^*} \right) \mathbf{S}, \quad \mathbf{D}^* = \left(\frac{U^*}{H^*} \right) \mathbf{D}, \quad r^* = R^* r, \quad z^* = H^* z \quad (4.1)$$

$$v_r^* = U^* v_r, \quad v_z^* = U^* \varepsilon v_z, \quad p^* = P_{\text{out}}^* + \left(\frac{\eta^* U^* R^*}{H^{*2}} \right) p, \quad t^* = \frac{R^*}{U^*} t \quad (4.2)$$

$$\sigma^* = H^* \sigma, \quad h^* = H^* h, \quad II_S^* = \left(\frac{\eta^* U^*}{H^*} \right) II_S, \quad II_D^* = \left(\frac{U^*}{H^*} \right) II_D, \quad (4.3)$$

and introduce the Reynolds and Bingham numbers

$$\text{Re} = \frac{\varrho^* U^* H^*}{\eta^*}, \quad \text{Bn} = \frac{\tau_o^* H^*}{\eta^* U^*}. \quad (4.4)$$

Mass balance becomes

$$\frac{\partial v_z}{\partial z} + \frac{\partial v_r}{\partial r} + \frac{v_r}{r} = 0, \quad (4.5)$$

while momentum balance becomes

$$\begin{cases} \varepsilon \text{Re} \left(\frac{\partial v_r}{\partial t} + v_r \frac{\partial v_r}{\partial r} + v_z \frac{\partial v_r}{\partial z} \right) = -\frac{\partial p}{\partial r} + \frac{\varepsilon}{r} \frac{\partial}{\partial r} (r S_{rr}) + \frac{\partial S_{rz}}{\partial z} - \varepsilon \frac{S_{\theta\theta}}{r}, \\ \varepsilon^3 \text{Re} \left(\frac{\partial v_z}{\partial t} + v_r \frac{\partial v_z}{\partial r} + v_z \frac{\partial v_z}{\partial z} \right) = -\frac{\partial p}{\partial z} + \frac{\varepsilon^2}{r} \frac{\partial}{\partial r} (r S_{rz}) + \varepsilon \frac{\partial S_{zz}}{\partial z}. \end{cases} \quad (4.6)$$

We also have

$$II_D = \frac{1}{2} \left[\left(\frac{\partial v_r}{\partial z} \right)^2 + \varepsilon^4 \left(\frac{\partial v_z}{\partial r} \right)^2 + 4\varepsilon^2 \left[\left(\frac{\partial v_r}{\partial r} \right)^2 + \left(\frac{v_r}{r} \right)^2 + \left(\frac{\partial v_r}{\partial r} \cdot \frac{v_r}{r} \right) + \frac{1}{2} \left(\frac{\partial v_r}{\partial z} \cdot \frac{\partial v_z}{\partial r} \right) \right] \right]^{1/2}$$

$$II_E = \frac{\Gamma}{\varepsilon} \left[\frac{1}{4} \left(\frac{\partial u_r}{\partial z} \right)^2 + \frac{\varepsilon^4}{4} \left(\frac{\partial u_z}{\partial r} \right)^2 + \varepsilon^2 \left[\left(\frac{\partial u_r}{\partial r} \right)^2 + \left(\frac{u_r}{r} \right)^2 + \left(\frac{\partial u_r}{\partial r} \cdot \frac{u_r}{r} \right) + \frac{1}{2} \left(\frac{\partial u_r}{\partial z} \cdot \frac{\partial u_z}{\partial r} \right) \right] \right]^{1/2}$$

where

$$\Gamma = \frac{k^* H^*}{\eta^* U^*} \quad (4.7)$$

is a dimensionless parameter expressing the ratio between the characteristic elastic stress and the characteristic viscous stress (see [24] for a detailed discussion on the physical meaning of Γ). Hence

$$\begin{cases} II_S > \text{Bn} \quad (\text{viscous}) & \implies II_D > 0, \\ II_S < \text{Bn} \quad (\text{linear elastic}) & \implies 2\Gamma II_E < \text{Bn}, \\ II_S = \text{Bn} \quad (\text{yield surface}) & \implies II_D = 0, \quad 2\Gamma II_E = \text{Bn}. \end{cases} \quad (4.8)$$

Accordingly the boundary conditions become

$$\begin{cases} v_z = \dot{h}(t), \quad v_r = 0, \quad (\text{no slip}), & \text{on } z = h(t), \\ v_z = 0, \quad S_{rz} = 0, \quad (\text{symmetry}), & \text{on } z = 0, \\ v_r = 0, \quad S_{rz} = 0, \quad (\text{symmetry}), & \text{on } r = 0, \\ p = 0 & \text{at } r = 1, \end{cases} \quad (4.9)$$

while conditions on the yield surface $z = \sigma(r, t)$ write

$$\left\{ \begin{array}{l} \llbracket v_z \rrbracket = \llbracket v_r \rrbracket = 0, \\ -\llbracket P \rrbracket \left[1 + \varepsilon^2 \left(\frac{\partial \sigma}{\partial r} \right)^2 \right] + \varepsilon^3 \left(\frac{\partial \sigma}{\partial r} \right)^2 \llbracket S_{rr} \rrbracket - 2\varepsilon^2 \left(\frac{\partial \sigma}{\partial r} \right) \llbracket S_{rz} \rrbracket + \varepsilon \llbracket S_{zz} \rrbracket = 0, \\ \llbracket S_{rz} \rrbracket + \varepsilon \left(\frac{\partial \sigma}{\partial r} \right) \left[\llbracket S_{zz} - S_{rr} \rrbracket - \varepsilon \left(\frac{\partial \sigma}{\partial r} \right) \llbracket S_{rz} \rrbracket \right] = 0. \end{array} \right. \quad (4.10)$$

Notice that, with the scaling introduced, $h(0) = 1$.

5 The leading order approximation

Because of the lubrication hypothesis we focus on the leading order terms only and, assuming $\text{Re} \leq \mathcal{O}(1)$, $\text{Bn} = \mathcal{O}(1)$, we neglect all the terms containing ε . We get

$$\left\{ \begin{array}{l} -\frac{\partial P^{(0)}}{\partial r} + \frac{\partial S_{rz}^{(0)}}{\partial z} = 0, \\ -\frac{\partial P^{(0)}}{\partial z} = 0, \end{array} \right. , \quad \left\{ \begin{array}{l} \llbracket v_r^{(0)} \rrbracket = \llbracket v_z^{(0)} \rrbracket = 0, \quad z = \sigma \\ \llbracket P^{(0)} \rrbracket = \llbracket S_{rz}^{(0)} \rrbracket = 0, \quad z = \sigma \end{array} \right.$$

with

$$II_S^{(0)} \Big|_{\sigma} = \text{Bn}, \quad \Rightarrow \quad II_D^{(0)} \Big|_{\sigma} = 0, \quad \Rightarrow \quad \frac{\partial v_r^{(0)}}{\partial z} \Big|_{\sigma} = 0,$$

and

$$\left\{ \begin{array}{l} v_z^{(0)} = \dot{h}, \quad z = h, \\ v_z^{(0)} = S_{rz}^{(0)} = 0, \quad z = 0, \\ v_r^{(0)} = S_{rz}^{(0)} = 0, \quad r = 0. \\ P^{(0)} = 0, \quad r = 1. \end{array} \right.$$

To keep notation simple, in what follows, we drop the superscript $^{(0)}$.

5.1 The viscous domain

In the viscous domain the problem is

$$\left\{ \begin{array}{l} -\frac{\partial P}{\partial r} + \frac{\partial}{\partial z} \left[\frac{\partial v_r}{\partial z} + \overbrace{\text{sgn} \left(\frac{\partial v_r}{\partial z} \right) \text{Bn}}^{S_{rz}} \right] = 0, \\ -\frac{\partial P}{\partial z} = 0, \end{array} \right.$$

We are looking for solutions with $\partial v_r / \partial z < 0$ since we are assuming no slip on the plate $z = h$, hence the sign in front of \mathbf{Bn} in the square bracket must be negative. Integrating with the specified boundary conditions we get

$$v_r = \frac{\partial P}{\partial r} \left[\frac{(z - \sigma)^2}{2} - \frac{(h - \sigma)^2}{2} \right]. \quad (5.1)$$

Now, exploiting mass conservation equation (4.5) we can easily find

$$r(\dot{h} - v_z) = \frac{(z - h)^2}{6} \frac{\partial}{\partial r} \left[r \frac{\partial P}{\partial r} (z - 3\sigma + 2h) \right]. \quad (5.2)$$

or equivalently

$$v_z = \dot{h} - \frac{(z - h)^2}{6r} \frac{\partial}{\partial r} \left[r \frac{\partial P}{\partial r} (z - 3\sigma + 2h) \right]. \quad (5.3)$$

As a consequence on $z = \sigma$ we get

$$\begin{cases} v_r|_\sigma = -\frac{\partial P}{\partial r} \frac{(h - \sigma)^2}{2}, \\ v_z|_\sigma = \dot{h} - \frac{(\sigma - h)^2}{6r} \left[2(h - \sigma) \frac{\partial}{\partial r} \left(r \frac{\partial P}{\partial r} \right) - 3r \frac{\partial P}{\partial r} \frac{\partial \sigma}{\partial r} \right], \end{cases} \quad (5.4)$$

Remark 1 We notice that the boundary condition $v_r = 0$ on $r = 0$ yields necessarily that $\partial P / \partial r = 0$ everywhere on $r = 0$, as expected because of symmetry.

5.2 The elastic region

In the elastic region we must distinguish between two cases

1. $\Gamma = O(1)$, i.e. viscous stress and elastic stress of the same order;
2. $\Gamma = O(\varepsilon)$, i.e. elastic stress much smaller than the viscous stress;

As shown in [24], Case 1 corresponds to negligible deformations, so that at the leading order the elastic part essentially behaves as a rigid solid. In this situation the model describes the squeezing of a classical Bingham fluid and we recover the well known paradox first described in [5].

For this reason we focus on Case 2 only, assuming that $\Gamma = \Theta \varepsilon$ with $\Theta = O(1)$.

To describe the dynamics in the elastic domain we refer to Fig. 2. In particular we suppose that there exists a domain

$$\Omega_c = \{0 \leq r \leq s(t); 0 \leq z \leq h(t)\}, \quad (5.5)$$

in which the material is everywhere unyielded⁴.

⁴In practice we suppose that the yield surface is always detached from $z = 0$ and $r = 0$.

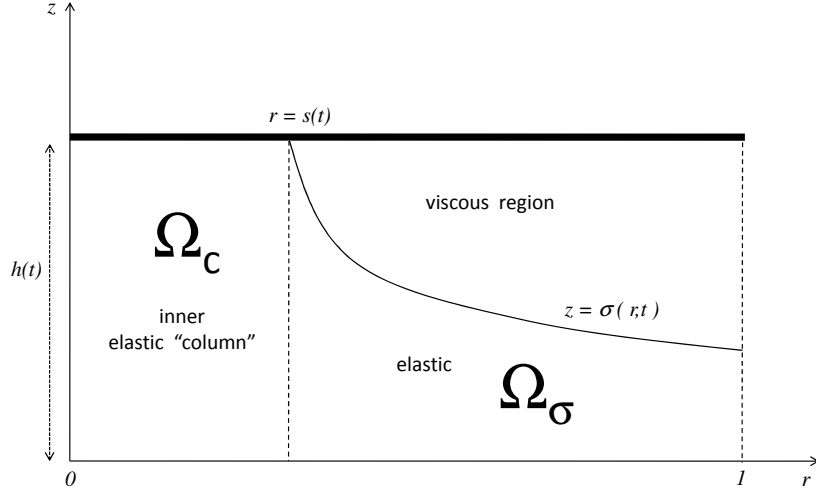


Figure 3: Domains Ω_c , Ω_σ and the viscous domain.

Referring to Fig. 3 we observe that Ω_c can be seen as an elastic inner column. In this region the material is everywhere elastic and the leading order problem becomes

$$\left\{ \begin{array}{l} -\frac{\partial P}{\partial r} + \Theta \frac{\partial^2 u_r}{\partial z^2} = 0, \\ -\frac{\partial P}{\partial z} = 0, \end{array} \right. \quad \left\{ \begin{array}{l} \frac{\partial u_r}{\partial z} \Big|_{z=0} = 0, \quad (\text{symmetry}), \\ u_r|_{z=h} = 0, \quad (\text{no-slip}), \\ P|_{r=1} = 0, \end{array} \right.$$

so that $P = P(r, t)$ and

$$u_r = \frac{\partial P}{\partial r} \left(\frac{z^2 - h^2}{2\Theta} \right), \quad \frac{\partial u_r}{\partial z} = \frac{\partial P}{\partial r} \frac{z}{\Theta}.$$

Because of symmetry $u_r|_{r=0} = 0$ so that $\frac{\partial P}{\partial r} \Big|_{r=0} = 0$. The stress at the wall $z = h(t)$ is given by

$$S_{rz}|_{z=h} = \Theta \frac{\partial u_r}{\partial z} \Big|_\sigma = \frac{\partial P}{\partial r} h.$$

Exploiting mass balance we write

$$\frac{\partial}{\partial z} \left(\frac{\partial u_z}{\partial t} \right) + \frac{1}{r} \frac{\partial}{\partial r} \left(r \frac{\partial u_r}{\partial t} \right) = 0,$$

$\underbrace{\hspace{10em}}_{\frac{\partial^2}{\partial r \partial t} (r u_r)}$

so that

$$\frac{\partial}{\partial z} \left(\frac{\partial u_z}{\partial t} \right) = -\frac{1}{r} \frac{\partial^2}{\partial r \partial t} \left[r \frac{\partial P}{\partial r} \left(\frac{z^2 - h^2}{2\Theta} \right) \right].$$

Integrating in z between 0 and h with the prescribed boundary conditions, we get

$$\Theta \dot{h} = \frac{1}{r} \frac{\partial^2}{\partial r \partial t} \left[\frac{h^3 r}{3} \frac{\partial P}{\partial r} \right].$$

Now we integrate along the radial coordinate, between 0 and r to find

$$\frac{3\Theta}{2} r \dot{h} = \frac{\partial}{\partial t} \left(h^3 \frac{\partial P}{\partial r} \right). \quad (5.6)$$

We assume that at time $t = 0$ the whole material is stress free, i.e.

$$P(r, 0) = \frac{\partial P}{\partial r} \Big|_{t=0} = 0$$

so that, integrating (5.6) in t and recalling that $h(0) = 1$, we find

$$\frac{\partial P}{\partial r} = \frac{3\Theta r}{2} \frac{(h-1)}{h^3}. \quad (5.7)$$

As a consequence the shear stress is

$$S_{rz} = \frac{3\Theta r z}{2} \frac{(h-1)}{h^3} < 0, \quad \Rightarrow \quad S_{rz}|_{z=h} = \frac{3\Theta r}{2} \frac{(h-1)}{h^2} < 0.$$

As previously observed, at the initial time $t = 0$ the system is at rest and the continuum is everywhere unyielded. As the plates begin to squeeze, $|S_{rz}(z, r, t)|$ increases attaining its maximum value in the corner $(h, 1)$. Therefore the appearance of the yield surface occurs when

$$|S_{rz}(z, r, t)| = \text{Bn}, \quad \Rightarrow \quad S_{rz}(h, 1, t) = -\text{Bn}.$$

As we keep on squeezing the stress becomes larger and the yielded region starts expanding, occupying the upper right corner of the domain as shown in Fig. 3. The onset of the yield surface is then placed on the upper plate $z = h(t)$ at location $r = s(t)$, which is defined by

$$-\text{Bn} = \frac{3\Theta s(t)}{2} \frac{(h-1)}{h^2} \quad \Rightarrow \quad s(t) = \frac{2\text{Bn}}{3\Theta} \frac{h^2(t)}{(1-h(t))} > 0.$$

Notice that nor s neither the yield surface σ are material. The function $s(t)$ is unbounded as $t \rightarrow 0$ and $\dot{s}(t) < 0$ (since $\dot{h} < 0$). Hence there will be a time interval $(0, T)$ in which $s(t) > 1$, i.e. in which the viscous phase has not yet appeared. At time T we have $s(T) = 1$, i.e. the viscous phase is appearing.

Remark 2 Assuming that $h(t)$ is strictly monotonically decreasing, the time T can be explicitly calculated setting $s(T) = 1$, which yields

$$2\text{Bn}h^2(T) + 3\Theta h(T) - 3\Theta = 0, \quad h(T) = \frac{-3\Theta + \sqrt{9\Theta^2 + 24\text{Bn}}}{4\text{Bn}} \in (0, 1),$$

so that

$$T = h^{-1} \left(\frac{-3\Theta + \sqrt{9\Theta^2 + 24\text{Bn}}}{4\text{Bn}} \right).$$

In particular, for any radius $r \in [0, 1)$, we can explicitly determine the time t_r in which the front s passes through r , i.e. $s(t_r) = r$. We find

$$t_r = h^{-1} \left(\frac{-3\Theta r + \sqrt{9\Theta^2 r^2 + 24\text{Bn}\Theta r}}{4\text{Bn}} \right) \quad (5.8)$$

So far we have solved the elastic problem in the column Ω_c given by (5.5). We now focus on the domain Ω_σ (see Fig. 3)

$$\Omega_\sigma = \{s(t) \leq r \leq 1; 0 \leq z \leq \sigma(t)\},$$

where we have to solve

$$\begin{cases} -\frac{\partial P}{\partial r} + \Theta \frac{\partial^2 u_r}{\partial z^2} = 0, \\ \frac{\partial u_r}{\partial z} \Big|_{z=0} = 0. \end{cases}$$

The radial displacement is

$$u_r = \frac{1}{\Theta} \left[\frac{\partial P}{\partial r} \frac{z^2}{2} + L(r, t) \right], \quad (5.9)$$

where L is unknown at this stage. In particular, since the radial velocity in Ω_σ is

$$\frac{\partial u_r}{\partial t} = \frac{1}{\Theta} \left[\frac{\partial^2 P}{\partial t \partial r} \frac{z^2}{2} + \frac{\partial L}{\partial t} \right],$$

exploiting $[[v_r]] = 0$ on σ , i.e.

$$\underbrace{\frac{\sigma^2}{2} \frac{\partial^2 P}{\partial r \partial t} + \frac{\partial L}{\partial t}}_{\Theta \frac{\partial u_r}{\partial t} \Big|_{r=\sigma^-}} = \underbrace{-\frac{\partial P}{\partial r} \frac{\Theta (h - \sigma)^2}{2}}_{\Theta v_r \Big|_{r=\sigma^+}},$$

we find $\frac{\partial L}{\partial t}$ and obtain

$$\frac{\partial u_r}{\partial t} = \frac{1}{\Theta} \frac{\partial^2 P}{\partial r \partial t} \left(\frac{z^2 - \sigma^2}{2} \right) - \frac{\partial P}{\partial r} \frac{(h - \sigma)^2}{2}. \quad (5.10)$$

We still have to derive the equation governing the dynamics of the yield surface $\sigma(r, t)$. To this aim we focus on the jump condition $[[S_{rz}]]_{z=\sigma} = 0$, that yields

$$\underbrace{\frac{\partial v_r}{\partial z} \Big|_\sigma}_{=0} - \text{Bn} = \Theta \frac{\partial u_r}{\partial z} \Big|_\sigma,$$

which, because of (5.9), gives⁵

$$\frac{\partial P}{\partial r} \sigma = -\text{Bn}. \quad (5.11)$$

Let us now use the global mass balance to derive the differential equation for σ . Considering any $r \in (s, 1)$, global mass conservation entails

$$\frac{d}{dt} [\pi r^2 h] = -2\pi r \left[\int_0^\sigma \frac{\partial u_r}{\partial t} dz + \int_\sigma^h v_r dz \right]. \quad (5.12)$$

⁵Condition (5.11) proves that the hypothesis that σ is detached from $r = 0$ and $z = 0$ is correct.

Plugging (5.1), (5.10) into (5.12) we find

$$\frac{\partial^2 P}{\partial r \partial t} = \frac{3\Theta}{\sigma^3} \left[\frac{r\dot{h}}{2} - \frac{\partial P}{\partial r} \frac{(h-\sigma)^2(2h+\sigma)}{6} \right]. \quad (5.13)$$

Next, exploiting (5.11), we obtain

$$\frac{\partial^2 P}{\partial r \partial t} = \frac{\partial \sigma}{\partial t} \frac{\text{Bn}}{\sigma^2}, \quad (5.14)$$

that we replace, along with (5.11), into (5.13), getting the following differential equation for σ

$$\frac{\partial \sigma}{\partial t} = \frac{3\Theta}{\sigma \text{Bn}} \left[\frac{r\dot{h}}{2} + \text{Bn} \frac{(h-\sigma)^2(2h+\sigma)}{6\sigma} \right]. \quad (5.15)$$

Equation (5.15) must be solved for any $r \in [s, 1]$ with the initial condition $\sigma(r, t_r) = h(t_r)$. Actually we can write the Cauchy problem for the whole interval $[0, 1]$

$$\begin{cases} \frac{\partial \sigma}{\partial t} = \frac{3\Theta}{\sigma \text{Bn}} \left[\frac{r\dot{h}}{2} + \text{Bn} \frac{(h-\sigma)^2(2h+\sigma)}{6\sigma} \right] \text{H}(t-t_r) + \text{H}(t_r-t)\dot{h} \\ \sigma(0, r) = 1, \end{cases} \quad (5.16)$$

where $\text{H}(x)$ is the Heaviside function

$$\text{H}(x) = \begin{cases} 1 & \text{if } x \geq 0, \\ 0 & \text{if } x < 0. \end{cases}$$

Indeed, replacing (5.15) with (5.16)₁, we have that for any fixed r the yielded region appears only when $s(t)$ crosses the position r , i.e. when $t \geq t_r$, with t_r defined in (5.8). Therefore, for $t \in [0, t_r]$, we have $\sigma(r, t) \equiv h(t)$ while for $t > t_r$ we recover (5.15), with the ‘‘initial condition’’ $\sigma(r, t_r) = h(t_r)$. The solution of (5.16) provides the function $\sigma(r, t)$ which, plugged into (5.11), allows to compute the pressure for $r \in [s, 1]$, namely

$$P(r, t) = \int_r^1 \frac{\text{Bn}}{\sigma(r', t)} dr', \quad r \in [s(t), 1]. \quad (5.17)$$

The pressure in $[0, s]$ is then found integrating (5.7) with the datum $P(s, t)$ obtained exploiting (5.17). We thus have

$$P(r, t) = \begin{cases} \int_r^1 \frac{\text{Bn}}{\sigma(r', t)} dr', & \text{if } r \in [s(t), 1], \\ \int_{s(t)}^1 \frac{\text{Bn}}{\sigma(r', t)} dr' - \frac{3\Theta}{4} \frac{(h(t)-1)}{h^3(t)} (s^2(t) - r^2), & \text{if } r \in [0, s(t)]. \end{cases} \quad (5.18)$$

6 Numerical simulation and discussion

In this section we plot the yield surface and the pressure for some prescribed squeezing velocity. We consider the following cases

$$(A), \quad h(t) = 1 - at, \quad \Theta = 3, \quad \text{Bn} = 1.5, \quad a = 1,$$

$$(B), \quad h(t) = \frac{1}{1 + at}, \quad \Theta = 2, \quad \text{Bn} = 2, \quad a = 3.5,$$

$$(c), \quad h(t) = 1 - \frac{2}{\pi} \arctan at, \quad \Theta = 2, \quad \text{Bn} = 1.5, \quad a = 1.2,$$

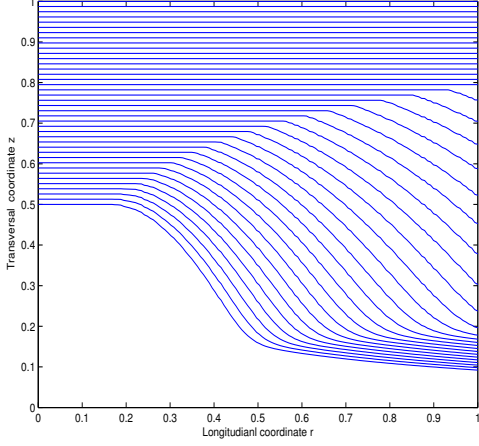


Figure 4: Yield surface case (A)

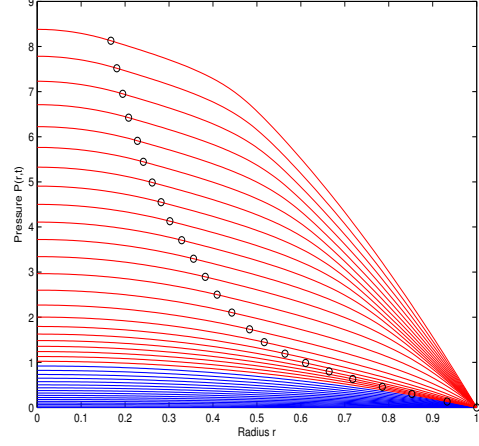


Figure 5: Pressure case (A)

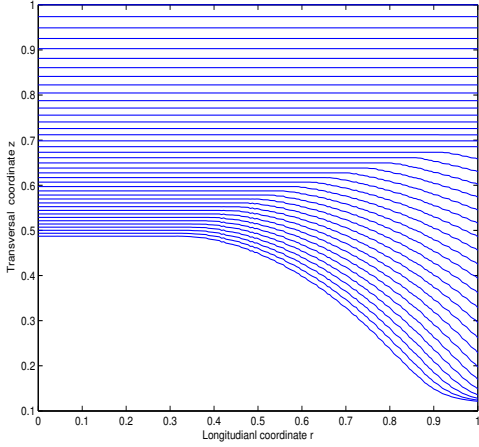


Figure 6: Yield surface case (B)

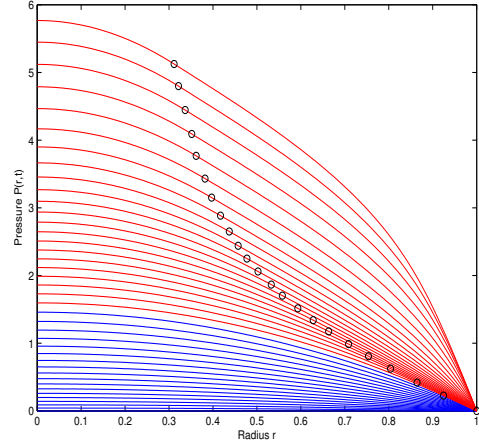


Figure 7: Pressure case (B)

For each case we plot the evolution of the yield surface $\sigma(r,t)$ (Fig. 4, 6, 8) and of the pressure $P(r,t)$ (Fig. 5, 7, 9). Plots are obtained integrating equation (5.15) and using (5.18)

In the plots of the pressure we indicate also the evolution of $r = s(t)$, i.e. the onset of the viscous phase. The red lines indicate pressure after time T , i.e. when the viscous phase has appeared. As one can notice the condition $\partial P / \partial r = 0$ is always met at $r = 0$.

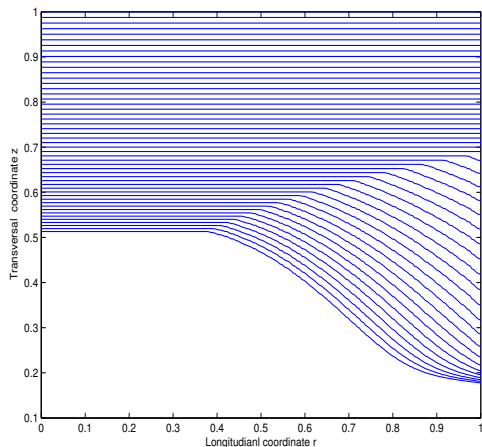


Figure 8: Yield surface case (C)

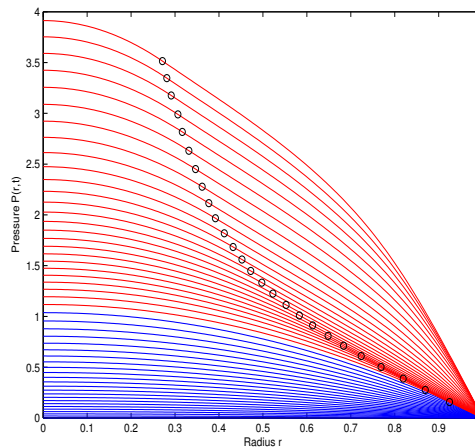


Figure 9: Pressure case (C)

7 Conclusion

We have studied the axisymmetric squeeze flow of a Bingham-type material in lubrication approximation. We have supposed that the unyielded part may undergo deformation and behaves like a linear elastic body. This modification of the classical Bingham constitutive relation, in which the unyielded part is modelled as a rigid body, has proven successful in overcoming the classical lubrication paradox arising in axisymmetric flows. We have focused on the leading order of the classical lubrication expansion and we have derived the evolution equation for the yield surface that separates the yielded and the unyielded domains.

Assuming that the system is initially at rest (and hence unyielded), we have found the time at which the viscous phase begins to appear on the upper right corner of the domain, showing that such a phase is always detached from the axis of symmetry of the flow. We have solved the problem numerically and we have plot the evolution of the main physical variables for different prescribed motions of the plates.

References

- [1] E. C. Bingham. *Fluidity and plasticity*. Volume 2. McGraw-Hill Book Company, Incorporated, 1922.
- [2] J. G. Oldroyd. “A rational formulation of the equations of plastic flow for a Bingham solid”. In: *Proc. Cambridge Philos. Soc.* 43 (1947), pages 100–105.
- [3] G.H. Covey and B.R. Stanmore. “Use of the parallel-plate plastometer for the characterisation of viscous fluids with a yield stress”. In: *Journal of Non-Newtonian Fluid Mechanics* 8.3 (1981), pages 249–260.
- [4] S. D. R. Wilson. “Squeezing flow of a Bingham material”. In: *Journal of Non-Newtonian Fluid Mechanics* 47 (1993), pages 211–219.
- [5] G. G. Lipscomb and M. M. Denn. “Flow of Bingham fluids in complex geometries”. In: *Journal of Non-Newtonian Fluid Mechanics* 14 (1984), pages 337–346.

- [6] A Putz, IA Frigaard, and DM Martinez. “On the lubrication paradox and the use of regularisation methods for lubrication flows”. In: *Journal of Non-Newtonian Fluid Mechanics* 163.1 (2009), pages 62–77.
- [7] IC Walton and SH Bittleston. “The axial flow of a Bingham plastic in a narrow eccentric annulus”. In: *Journal of Fluid Mechanics* 222 (1991), pages 39–60.
- [8] N.J. Balmforth and R.V. Craster. “A consistent thin-layer theory for Bingham plastics”. In: *Journal of non-newtonian fluid mechanics* 84.1 (1999), pages 65–81.
- [9] I. A. Frigaard and D. P. Ryan. “Flow of a visco-plastic fluid in a channel of slowly varying width”. In: *Journal of Non-Newtonian Fluid Mechanics* 123.1 (2004), pages 67–83.
- [10] D.K Gartling and N. Phan-Thien. “A numerical simulation of a plastic fluid in a parallel-plate plastometer”. In: *Journal of non-Newtonian fluid mechanics* 14 (1984), pages 347–360.
- [11] D. N. Smyrniotis and J. A. Tsamopoulos. “Squeeze flow of Bingham plastics”. In: *Journal of Non-Newtonian Fluid Mechanics* 100.1 (2001), pages 165–189.
- [12] T. C. Papanastasiou. “Flows of materials with yield”. In: *Journal of Rheology* 31.5 (1987), pages 385–404.
- [13] JD Sherwood and D Durban. “Squeeze-flow of a Herschel–Bulkley fluid”. In: *Journal of Non-Newtonian Fluid Mechanics* 77.1 (1998), pages 115–121.
- [14] JD Sherwood and D Durban. “Squeeze flow of a power-law viscoplastic solid”. In: *Journal of non-newtonian fluid mechanics* 62.1 (1996), pages 35–54.
- [15] P. Coussot. “Yield stress fluid flows: a review of experimental data”. In: *Journal of Non-Newtonian Fluid Mechanics* 211 (2014), pages 31–49.
- [16] J. Engmann, C. Servais, and A. S. Burbidge. “Squeeze flow theory and applications to rheometry: A review”. In: *Journal of Non-Newtonian Fluid Mechanics* 132.1-3 (2005), 1–27.
- [17] E Mitsoulis and A Matsoukas. “Free surface effects in squeeze flow of Bingham plastics”. In: *Journal of non-newtonian fluid mechanics* 129.3 (2005), pages 182–187.
- [18] E. Mitsoulis. “Flows of viscoplastic materials: models and computations”. In: *Rheology Reviews* 135178 (2007).
- [19] IA Frigaard and C Nouar. “On the usage of viscosity regularisation methods for viscoplastic fluid flow computation”. In: *Journal of Non-Newtonian Fluid Mechanics* 127.1 (2005), pages 1–26.
- [20] Neil J Balmforth, Ian A Frigaard, and Guillaume Ovarlez. “Yielding to stress: recent developments in viscoplastic fluid mechanics”. In: *Annual Review of Fluid Mechanics* 46 (2014), pages 121–146.
- [21] L. Fusi, A. Farina, F. Rosso, and S. Roscani. “Pressure driven lubrication flow of a Bingham fluid in a channel: A novel approach”. In: *Journal of Non-Newtonian Fluid Mechanics* 221 (2015), pages 66–75.
- [22] L. Fusi, A. Farina, and F. Rosso. “Planar Squeeze Flow of a Bingham Fluid”. In: *to appear on Journal of Non-Newtonian Fluid Mechanics* (2015), in.
- [23] L. Muravleva. “Squeeze plane flow of viscoplastic Bingham material”. In: *Journal of Non-Newtonian Fluid Mechanics* 220 (2015), pages 148–161.
- [24] L. Fusi, A. Farina, and F. Rosso. “Flow of a Bingham-like fluid in a finite channel of varying width: a two-scale approach”. In: *Journal of Non-Newtonian Fluid Mechanics* 177-178 (2012), 76–88.
- [25] L. Fusi and A. Farina. “An extension of the Bingham model to the case of an elastic core”. In: *Advances in Mathematical Sciences and Applications* 13.1 (2003), pages 113–163.

- [26] A. S. Yoshimura and R. K. Prud'homme. "Response of an elastic Bingham fluid to oscillatory shear". In: *Rheologica Acta* 26.5 (1987), pages 428–436.